Available online at www.sciencedirect.com
SCIENCE DIRECT
Carbohydrate Polymers 64 (2006) 239–246
Carbohydrate Polymers
www.elsevier.com/locate/carbpol

Dissolution kinetics of guar gum powders—III. Effect of particle size

Qi Wang [a,b], Peter R. Ellis [a], Simon B. Ross-Murphy [c,*]

[a] Nutritional Sciences Research Division, Biopolymers Group, King's College London, Franklin-Wilkins Building, 150 Stamford Street, London SE1 9NH, UK
[b] Food Research Program, AAFC, 93 Stone Road West, Guelph, Canada N1G 5C9
[c] Pharmaceutical Sciences Research Division, Molecular Biophysics Group, King's College London, Franklin-Wilkins Building, 150 Stamford Street, London SE1 9NH, UK

Received 26 October 2005; received in revised form 17 November 2005; accepted 21 November 2005
Available online 18 January 2006

Abstract

The functional properties of guar gum, which are of considerable importance in biological, industrial and biotechnology processes, are crucially dependent on the rate and extent of dissolution in an aqueous solvent. This work investigates the effect of particle size on the hydration rate of guar gum powders over a wide range of particle sizes. A logarithmic model described in a previous paper for studying the hydration kinetics of commercial guar flours was not applicable for some of these samples, because they were of a very much larger particle size, outside the usual commercial range. For this reason, a new approach was developed to describe the hydration process of these guar gum granules. It was found to be suitable for describing the hydration process of guar powders with a wide range of particle size, by introducing size-dependent hydration indices. This approach involves the construction of a master plot, but the 'shift factors' are related to particle size and the hydration time. This model consequently allows some new physical insights to be developed.

Keywords: Guar gum; Galactomannan; Dietary fibre; Soluble fibre; Non-starch polysaccharides; Hydration; Dissolution; Ultimate viscosity; Particle size effects

1. Introduction

The property of some non-starch polysaccharides (NSPs), such as guar galactomannan, to form molecular solutions when dispersed in water is of importance in a number of technological processes. In the pharmaceutical sector, for example, the functional properties of these polysaccharides are of primary importance for controlling the release of drugs in the gastrointestinal tract (i.e. drug delivery systems) (Chourasia & Jain, 2004; Friend, 2005; Montejo, Barcia, Fernandez-Carballido, & Molina-Martinez, 2004). In the oil industry, guar gum and its derivatives are major ingredients in drilling muds and fingering fluids (Goel, Shah, & Asadi, 2000; Kesavan & Prudhomme, 1992; Perez, Siquier, Ramirez, Muller, & Saez, 2004; Zhou & Shah, 2004), and in the textile industry guar solutions help to improve printing quality (Kesavan & Prudhomme, 1992; Schneider & Sostar-Turk, 2003; Turk & Schneider, 2000). Nutraceutical preparations that contain one or more water-soluble NSPs as the bioactive ingredient are promoted commercially for their potential health benefits (e.g. bulk-forming laxative and blood glucose-lowering effects) (Ellis & Morris, 1991; Guo, Skinner, Harcum, & Barnum, 1998; Patrick, Gohman, Marx, DeLegge, & Greenberg, 1998; Slavin & Greenberg, 2003). Water-soluble NSPs are often referred to generically as *soluble fibre* in the medical and nutritional literature. Some of these fibre preparations are currently available on prescription in the UK (Joint Formulary Committee, 2005). Moreover, foods and diets that contain soluble fibre from oats and psyllium seeds have received official approval by the US Food and Drugs Administration and permit a claim to be made about their potential use in reducing the risk of heart disease (US Food & Drug Administration, 1994). This health claim is based on the results of clinical trials demonstrating the blood cholesterol-lowering property of soluble fibre in human subjects (Anderson et al., 2000; Braaten et al., 1994).

It is generally recognised that the beneficial biological properties of soluble fibre are strongly dependent on the capacity of the water-soluble NSPs to hydrate and increase the viscosity of the luminal contents of the gastrointestinal tract (Jenkins et al., 1978; Wood et al., 1994). For instance, the blood glucose-lowering effect of guar gum is most likely a result of viscosity development in the stomach and small intestine in the early post-prandial period, i.e. the first hour

* Corresponding author. Tel.: +44 20 7848 4081; fax: +44 20 7848 4082/4500.
E-mail address: simon.ross-murphy@kcl.ac.uk (S.B. Ross-Murphy).

0144-8617/$ - see front matter © 2005 Elsevier Ltd. All rights reserved.
doi:10.1016/j.carbpol.2005.11.032

(Ellis, Roberts, Low, & Morgan, 1995; Ellis, Wang, Rayment, Ren, & Ross-Murphy, 2001). Indeed, it has been known for some time that the rate and degree of hydration of guar gum are critical variables in influencing its biological activity (Ellis, Morris, & Low, 1986; O'Connor, Tredger, & Morgan, 1981). Moreover, the poor clinical performance of some pharmaceutical preparations of guar gum in attenuating post-prandial glycaemia may simply be due to their inability to hydrate and increase digesta viscosity in the gut lumen (Ellis & Morris, 1991).

A number of factors are known to influence the hydration or dissolution process including the molecular weight and concentration of galactomannan in the guar powder (Wang, Ellis, & Ross-Murphy, 2002, 2003), and also the environmental conditions (temperature and pH) and the presence of co-solutes such as sucrose and salts) (Carlson, Ziengenfuss, & Overton, 1962; Ellis et al., 2001; Wang, Ellis, & Ross-Murphy, 2000; Whister & Hymowitz, 1979). Over and above this, our earlier work has established that the major determinant of hydration kinetics is particle size, which reflects the changes in surface area exposed to water. Not surprisingly, large variations in the hydration rate of guar powders and pharmaceutical preparations (e.g. tablets and granules) were reported in a number of studies (Ellis, Dawoud, & Morris, 1991; Ellis & Morris, 1991; O'Connor et al., 1981; To, Mitchell, Hill, Bardon, & Matthews, 1994). Two of these studies clearly showed an inverse relationship between dissolution rate and particle size (Ellis & Morris, 1991; To et al., 1994). In one recent paper, we described a novel method for hydrating guar gum powders and determining their dissolution kinetics by using a clearly defined viscosity criterion as an index of hydration (Wang et al., 2002). An important objective of this study was to evaluate the fitting of the hydration kinetic data to three empirical models, one of which, a logarithmic function, proved to be the most suitable for describing the behaviour of guar gum powders. A second paper made use of this model to investigate the effects of polymer concentration and molecular weight on the hydration index ($t_{0.8}$), which was derived from the logarithmic function and defined as the time taken for viscosity to reach 80% of ultimate viscosity (Wang et al., 2003).

As a natural extension of these two recent studies, the current paper reports the effects of particle size on the hydration rate of guar gum. It appears that the logarithmic model developed in our previous papers is eminently suitable for the hydration process of guar gum powders, where the mean particle size is ~50 to 70 μm (Wang et al., 2002, 2003). However, this model appears not to be as applicable to guar samples of particle size larger than ~80 μm (Wang et al., 2002). Furthermore, the logarithmic model requires that the ultimate viscosity of fully hydrated samples must be measurable. Because of this, any factor that changes the ultimate viscosity, such as time/temperature-induced polymer degradation, will influence the extrapolated result. In this paper, we have applied an additional model to the hydration data obtained using guar samples of different particle sizes (up to a mean value of ~500 μm) and we have compared these to the fitting of the same data to the logarithmic function.

2. Experimental

2.1. Materials

Six guar gum samples with a wide range of particle size (70–470 μm) were prepared directly from the same batch of guar seed endosperm (commercially referred to as 'splits') (Ellis et al., 2001). This approach helped to minimise differences in physical and chemical properties such as molecular weight and galactomannan content, and therefore, properties other than particle size were well controlled. All six samples were prepared from the endosperm splits using a standard milling procedure. Special care was taken to minimise the possibility of depolymerisation of the galactomannan by preventing the sample from over-heating during the milling process. The control of particle size was achieved by controlling the total transit time through the mill, i.e. batch time × number of passages. The moisture contents of the samples were adjusted to approximately the same level (11.2 ± 0.7%) before performing the hydration experiments. This was achieved by placing the samples in a container, which was then left in a sealed incubator containing a beaker of saturated sodium chloride solutions for about 48 h at 27 °C.

2.2. Methods for chemical analysis of guar gum

The moisture content was measured after heating the samples in a forced air (fan-assisted) oven (Gallenkamp Hotbox) at 104 °C for 16 h. The galactomannan content of each guar gum sample was analysed using the Englyst method (Englyst, Quigley, Hudson, & Cummings, 1992), which is performed by gas–liquid chromatography following acid hydrolysis and derivatisation of the carbohydrates to alditol acetates. In our experiments, we slightly modified this method by employing an extended hydration time for the guar samples in phosphate buffer (Wang et al., 2003).

2.3. Methods for physical characterisation of guar gum

Intrinsic viscosity was measured using a dilute solution capillary viscometer (Ubbelohde type) as detailed in our previous paper (Wang et al., 2002). The viscosity–average molecular weight (M_v) was estimated by use of an appropriate Mark–Houwink relationship (Robinson, Ross-Murphy, & Morris, 1982), and we assume that weight–average molecular weight, $M_w \approx M_v$. The guar gum samples used for intrinsic viscosity measurements were purified by a method described in detail in previous publications (Rayment, Ross-Murphy, & Ellis, 1995).

Particle sizes of the samples were measured either by a Malvern 2600 Laser Diffraction Sizer (Malvern Instruments Ltd, Worcestershire, WR14 1XZ, UK), or by a standard sieving method (Lauer, 1966). The former has been described in the previous paper (Wang et al., 2002). Sieving analysis was

carried out on a mechanical sieve shaker (Endecott test sieve shaker, Endecotts Ltd, London SW19, UK). A minimum of five sieving stages were selected so as to have the median average of particle size located at the central sieve (Jelinek, 1974). The sieves used in this experiment form the series of $d_n = \sqrt{2}d_{n-1}$, where $d_{i,i=1,n}$ is the average pore aperture. Each sample (30 g) was placed on the top coarse sieve (200 mm in diameter), and the sample was automatically sieved for 1 h. Then a soft brush was used to help the fine particles pass through the sieves. The sieving process was assumed complete when the rate of weight reduction for each mesh was less than 0.2 g/min. Each sample was analysed in duplicate. The samples were also examined by scanning electron microscopy (SEM) to provide further information about the shape and size of the guar gum particles; details of the SEM method are found in Wang et al. (2003).

In characterising more complex particles, both surface area and volume are important parameters. The surface area per unit volume is called the volume-specific surface (S_v). In sieving analysis, S_v and the mean diameter (d_{sv}) can be obtained by

$$d_{sv} = \frac{\alpha_{sv}}{S_v} \tag{1a}$$

$$S_v = \alpha_{sv} \sum \frac{W_r}{d_{a,r}} \tag{1b}$$

where w_r is the fractional weight residing between two sieves of average aperture $d_{a,r}$ (Allen, 1990) and α_{sv} is the surface–volume shape coefficient. $\alpha_{sv}=6$ for spheres and increases when the particles become less shape homogeneous, e.g. rod-like or 'flaky'. The complete list of standards may be obtained from British Standards BS4359 (British Standards Institution, 1970).

If particle size and shape analysis is carried out using two different techniques, the two results can be brought into coincidence by multiplying by a shape factor, assuming that the particle shape does not change with particle size (Allen, 1990). In the present study, one of the samples of medium size (sample 5) was analysed using both sieving and laser diffraction methods (Malvern instrument). The ratio ψ_d (i.e. the shape factor) was obtained from these two measurements as follows:

$$\psi_d = \frac{d_s}{d_m} \tag{2}$$

where d_s and d_m are the characteristic size obtained by sieving and Malvern techniques, respectively. This ratio was applied to convert the results obtained by the Malvern instrument to that of the standard sieving results for samples 5 and 6. In other words, a diameter determined by laser diffraction technique multiplied by the ratio ψ_d would yield the sieving diameter.

2.4. Hydration method

The hydration method used in this study has been described in detail in the previous publications (Wang et al., 2002, 2003). In summary, accurately weighed samples of guar gum were dispersed in 500 ml distilled water in a glass jar, which was then placed in a mixing incubator and rotated end-over-end at a constant rotational velocity (10 rpm) at 25 °C. The guar gum concentration used was 1.0% (w/v) of dry matter content, based on the final solution concentration. The hydration rate of the guar gum samples was monitored by taking viscosity measurements at several time intervals over a period of 6 h, and then one more time following homogenisation (Ultra-Turrax mixer) for approximately 6 min and further hydration for 3 h at 40 °C (the latter reading is referred to as the 'ultimate viscosity'). Viscosity was measured by a Rheometrics Fluid Spectrometer (RFS II; Rheometric Scientific, now TA Instruments, Rheometrics Series, Piscataway, NJ, USA) with a plate–plate geometry (50 mm in diameter, 1 mm gap). The rationale for employing this geometry rather than the more usual cone/plate system is discussed elsewhere (Wang et al., 2002). Zero-shear viscosity was estimated as the average value of the first four shear rates starting at the lowest shear rate. During each experiment five measurements were recorded per decade, typically from ~0.01 to 1000 s^{-1}.

3. Results

3.1. Characterisation of guar gum samples

The particle shapes of all the guar gum samples were broadly similar to each other, as can be seen in the SEM images of a selection of samples with a broad range of particle sizes (Fig. 1a–c). By examining the shapes of the powder particles using SEM, a surface–volume shape coefficient $\alpha_{sv}=10$ was selected in reference to British Standard 4359 (British Standards Institution, 1970). This value was used for the calculation of the mean particle size (d_{sv}) and volume-specific surface (S_v) according to Eqs. (1a) and (1b).

The particle sizes of samples 1–4 were determined directly from the sieving method and those of samples 5 and 6 were measured using the Malvern technique and converted to the equivalent sieving data using the shape factor ψ_d. As an example, Fig. 2a illustrates the conversion of data for sample 5 obtained from the Malvern instrument to that of the sieving technique. The median size (the 50% size on the cumulative frequency curve) of sample 5 from the Malvern ($d_{m,0.5}$) and sieving ($d_{s,0.5}$) methods were 75.6 and 112.5 μm, respectively. From these two values the shape factor, ψ_d, was calculated:

$$\psi_d = \frac{d_{s,0.5}}{d_{m,0.5}} = \frac{112.5}{75.6} = 1.49 \tag{3}$$

The results of particle size analyses for all six guar samples are presented in the form of cumulative undersize frequency curve expressed as a percentage in Fig. 2b. From Eqs. (1a) and (1b) the mean diameter (d_s) and volume-specific surface (S_{sv}) were calculated and tabulated in Table 1. Other chemical and physical characteristics including moisture and galactomannan contents and intrinsic viscosity were found to be similar for all the samples (Table 1).

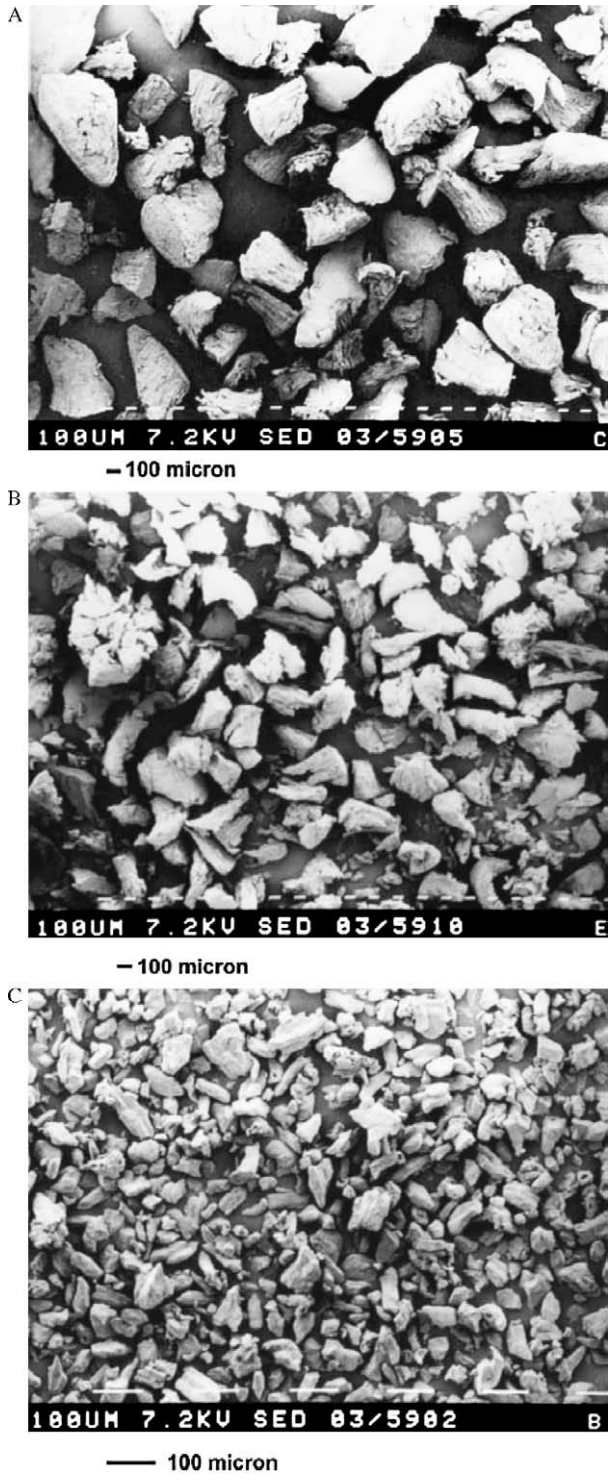

Fig. 1. Micrographs produced by scanning electron microscopy of guar gum samples of different particle size: (a) sample 1, (b) sample 3, and (c) sample 6. All scale bars = 100 μm.

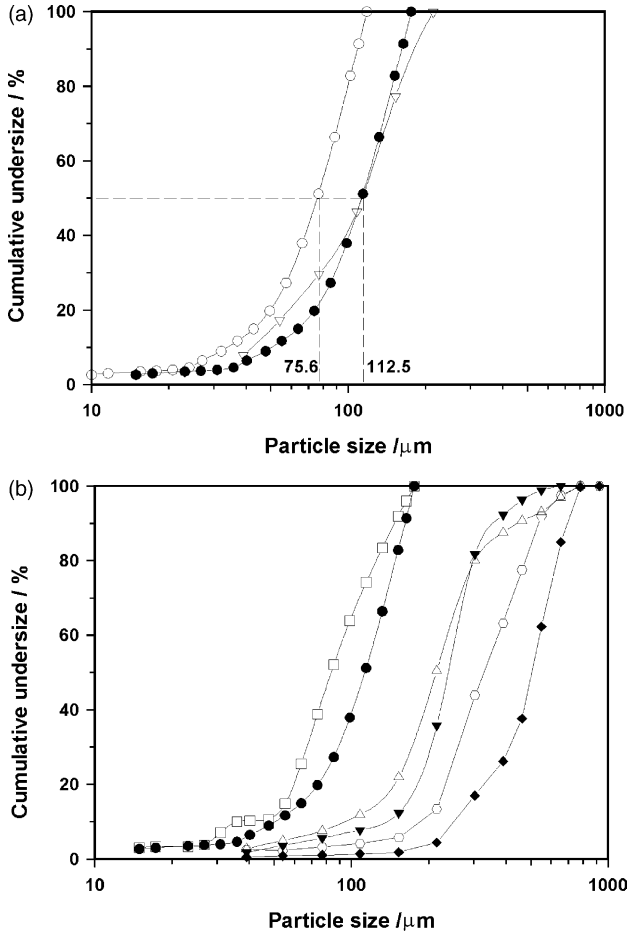

Fig. 2. (a) Converting particle sizing distribution of sample 5 obtained from Malvern technique to that of sieving analysis using ratio ψ_d (see Eqs. (2) and (3)), where $d_{s,0.5} = 112.5$ and $d_{m,0.5} = 75.6$ are the median size of sample 5 obtained by sieving and Malvern methods, respectively. Symbols: sieving method, open triangle; Malvern method, open circle; converted data, filled circles (b) particle size cumulative percentage curves for samples 1–6. Data of samples 5 and 6 were produced from Malvern measurements and converted to sieving data using ratio ψ_d. The rest of the data were obtained by sieving analysis. Symbols: sample 1, filled diamond; sample 2, open hexagon; sample 3, filled triangle down; sample 4, open triangle up; sample 5, filled circle; sample 6, open square.

3.2. Master plot method and effect of particle size on hydration rate

Fig. 3 shows the hydration profiles of all six samples. As mentioned above, in our earlier work on a more restricted sample size range, we used a logarithmic model to describe the hydration process (Wang et al., 2002)

$$\ln\left(\frac{1-\eta_t}{\eta_\infty}\right) = b + k \ln t \tag{4}$$

where η_t is the apparent zero-shear viscosity at time t, η_∞ is the ultimate viscosity of the dispersion and b and k are constants for a given sample hydrated at specified conditions. Eq. (4) implies that a plot of $\ln(1-\eta_t/\eta_\infty)$ versus $\ln t$ should yield a straight line, with hydration constants b and k extracted from the intercept and slope of this plot, respectively. However, it became clear that this approach failed progressively when larger particle sizes were considered. Among the six samples tested, the logarithmic model was found to fit the hydration profiles of only sample 6 (Fig. 4a), which has the smallest mean particle size (Table 1). Fig. 4b illustrates the failure of this

Table 1
Moisture and galactomannan (GM) contents, intrinsic viscosity [η] and mean particle size (d_{sv}) of guar gum samples of different particle size (numbered 1–6)

Samples	1	2	3	4	5	6
Moisture (%)	11.4	11.5	11.8	11.8	10.3	10.5
[η] (dl/g)	16.1	16.7	16.9	16.4	17.3	16.0
GM (%)	86.2	87.5	86.2	87.9	85.3	89.4
d_{sv} (μm)	477	300	223	194	113	74

Values are means of duplicates.

logarithmic model, here illustrated with data for sample 1. It is quite apparent that this model cannot be applied when the data produce a decrease in the slope (cf. Fig. 3). Instead of adopting the method above, we investigated alternative approaches. Clearly a simple, single-process, kinetic model for the hydration behaviour will not be appropriate, because such a model would tend to have a maximum slope (rate of hydration) at time 0. This is not at all what is seen, and clearly the development of a more rigorous model would necessarily entail introducing a number of extra parameters.

If Fig. 3 is plotted in double log form (Fig. 5a), the new representation immediately suggests that all the data follow a single fundamental hydration process, and one in which the effect of increasing particle size is to increase the time for 'total' hydration (Table 2). Initially this would appear to be a gross simplification, but it is an assumption worth pursuing. By first defining the largest particle size data to have a scale factor of unity, then all the subsequent data can be shifted (horizontally) by multiplying the actual hydration times by an arbitrary factor. For example, the shift factor for the smallest particle size appears to be ≈130, with appropriate intermediate values for the other samples.

What this means in practice is that the viscosity developed by a sample hydrated for say 1 h, for the smallest particle size, is, within the limitations of this approach, the same as that for the largest particle size sample when hydrated for 130 h, i.e.

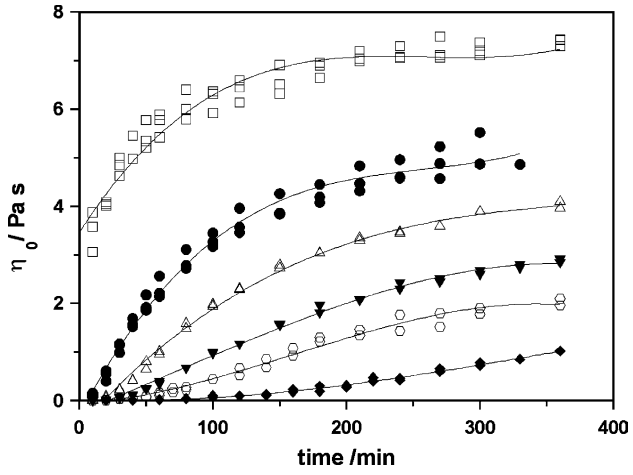

Fig. 3. Zero shear viscosity plotted against hydration time for all six samples showing replicate data. Symbols are as Fig. 2b. Curves are cubic polynomial regressions to the means of the replicate measurements.

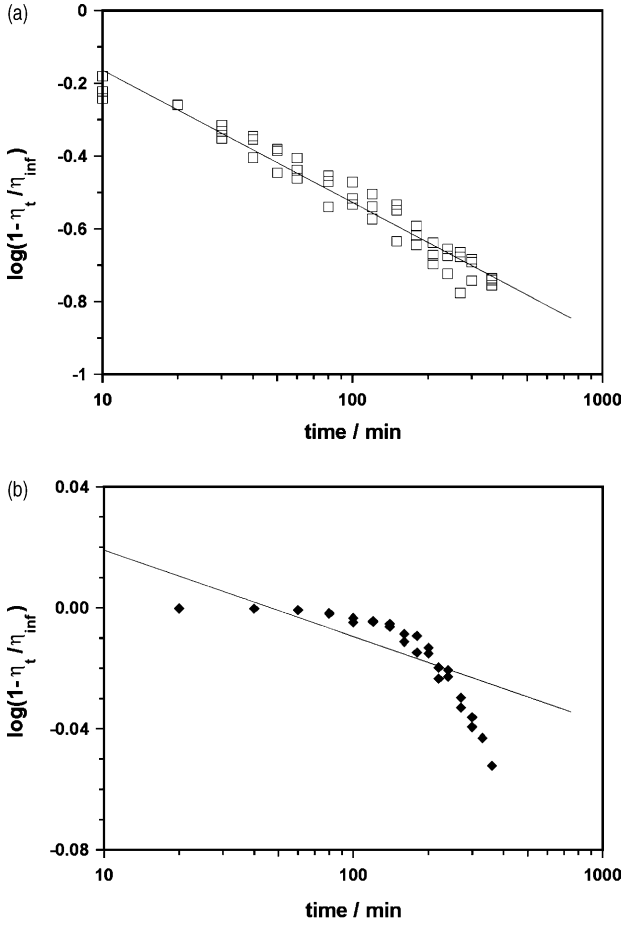

Fig. 4. (a) The logarithmic model (Eq. (4)) applied to the hydration profile of the smallest particle size sample (sample 6) and (b) the same plot for the largest particle size material (sample 1).

≈5.4 days. Of course the assumption implicit in this approach is that the particle hydrates in a uniform manner and, in particular, does not fragment during the dissolution process. Such a mechanism of fragmentation and dispersion would obviously tend to accelerate the overall hydration since, given the same total volume, one very large particle would tend to hydrate more slowly than a number of smaller particles.

With the lack of fragmentation assumption implicit, and at the low hydration shear rates employed in our experiments, one would expect the overall rate of hydration to depend on the surface area, for homogeneously shaped material, and on the volume for more tessellated and complex geometry particles. This would suggest that the exponent for the timescale for hydration would lie somewhere between 2 (since area $\propto d^2$) and 3 (volume $\propto d^3$). If we plot the time shift factor used in passing from Fig. 5a to Fig. 5b against particle size, we obtain the linear plot seen in Fig. 6, and gratifyingly the appropriate exponent, calculated from the linear slope, is $(-)2.46 \pm 0.32$ (SE). Here, the negative exponent merely reflects the fact that perhaps contrary to intuition, we defined the shift factor for the largest sample to be unity, but we did this in order to reflect an increase of the effective time-scale for the smallest sample. This is, of

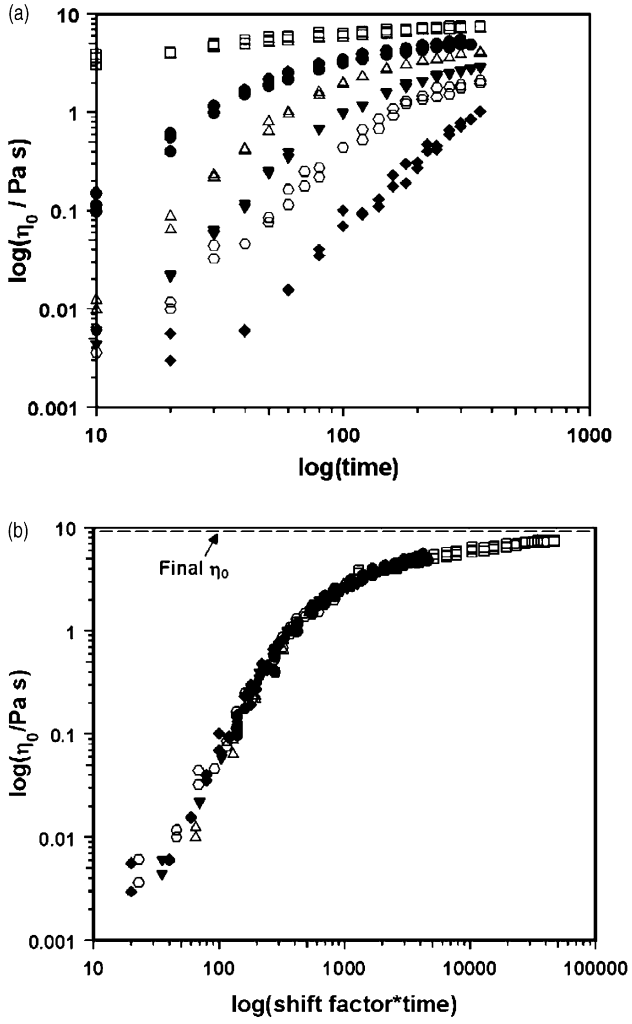

Fig. 5. (a) Log viscosity plotted versus log hydration time for the data of Fig. 3, and (b) corresponding master curve of log viscosity versus scaled time, produced from the above data by applying a time shift-factor. Symbols as Fig. 2b. Dotted line represents the mean 'fully hydrated' viscosity for all samples (cf. Table 2).

course, an arbitrary decision, but one that appears, to us, to be quite rational. The advantage of such a master curve approach is now quite clear in that we can interpolate the maximum (and intermediate) hydration time(s) for any particle size within this size range ~70–500 μm, quite readily, and even use it to extrapolate to more extreme ranges.

Table 2
Particle size, viscosity after 360 min hydration and final viscosity

Samples	1	2	3	4	5	6
d_{sv} (μm)	477	300	223	194	113	74
η_{360} (Pa s)	1.0^{a}_{2}	2.0_{3}	2.8_{8}	4.0_{3}	4.8^{b}_{6}	7.3_{8}
η_{∞} (Pa s)	9.5_{9}	9.1_{8}	8.7_{7}	9.5_{3}	9.1_{1}	9.0_{1}

Values are means of 2–3 replicates.
[a] Subscripted figures indicate that measured data are not significant to better than ± ~5%.
[b] Value measured after 330 min.

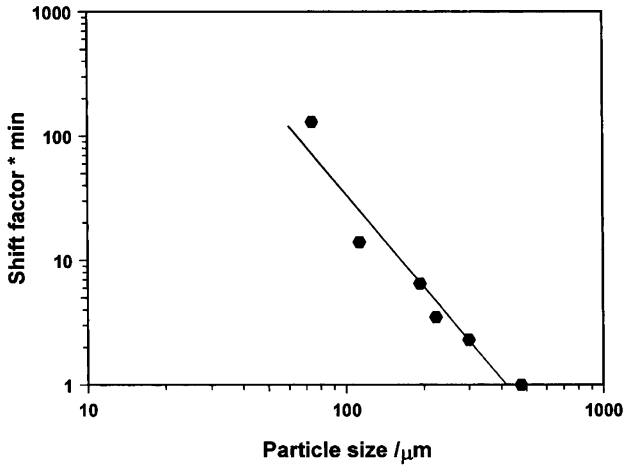

Fig. 6. The time shift factor used in constructing Fig. 5b plotted versus particle size. The fitted line has a slope of -2.46 ± 0.32 (standard error). The r^2, (correlation coefficient)^2 is 0.94.

4. Discussion

Currently there are very few models that can provide a relationship between particle size and hydration rate, and most of these, as we discussed in our earlier papers, can be applied only in a comparatively limited range of particle size. We feel that the new logarithmic superposition model has some advantages, not only because it is capable of extending the particle size range, but also because the hydration time shift factors relate quite sensibly to change in particle size. The comparative simplicity of this approach makes it potentially very attractive, and may prove of value in correlating viscosity–time growth for other particulate systems, say in the pharmaceutical and oil extraction industries.

Finally, this raises the question of the relevance of the hydration shear rate employed here to the much higher rates employed, for example in industrial processing; how could these change the results obtained? In the latter case what may be just as significant as the time for hydration is the integral strain exerted during the hydration stages (i.e. approximately the product of the hydration strain rate and the time). We surmise that in the absence of fragmentation, the relationship is less than linear, i.e. doubling the 'hydration shear rate' will not half the time to hydration, but decrease it by a smaller fraction. However, larger shear rates will also tend to encourage fragmentation, so that the net effect may not be far from the original assumption of integrated strain. In any case this suggests a whole catalogue of further experiments that could be well worth pursuing.

5. Conclusions

For guar gum powders with a mean particle size <80 μm the logarithmic model is extremely useful for describing the hydration kinetic data, as discussed in our previous papers (Wang et al., 2002, 2003). For larger size samples, the new method was found to be more suitable for comparing the

hydration rate of several samples that could not be fitted by this, especially when the ultimate viscosity varies between samples or is difficult to determine. Using this approach a relationship between time for hydration and mean particle size was demonstrated in the particle size range 70–500 μm. The application of the logarithmic superposition method to an *in vitro* digestion model for studying the viscosity development of foods/diets containing water soluble NSPs is planned. Moreover, the model has much broader relevance to the hydration of other materials, which, would in turn, suggest wider industrial interests.

Acknowledgements

The authors gratefully acknowledge the financial support from Danisco A/S, Copenhagen, Denmark (formerly Rhodia Food Ingredients, Boulogne-Billancourt cedex, France, and previously Meyhall Chemical AG Kreuzlingen, Switzerland). We are especially grateful to Mr W.C. Wielinga (formerly Meyhall Chemical AG) for preparing the guar gum samples. We would also like to thank colleagues at King's College London, Dr A. Brain for his expert assistance with the SEM work, and Mr V. Dawes, and Dr X.M. Zeng for their help and advice with the methods for determining the particle size distribution of the guar gum samples. The Rheometrics RFSII was purchased courtesy of the BBSRC, under grant F01033.

References

Allen, T. (1990). Particle size, shape and distribution. In *Particle size measurement*. London: Chapman & Hall.

Anderson, J. W., Davidson, M. H., Blonde, L., Brown, W. V., Howard, W. J., Ginsberg, H., et al. (2000). Long-term cholesterol-lowering effect of psyllium as an adjunct to diet therapy in the treatment of hypercholesterolaemia. *American Journal of Clinical Nutrition*, *71*(346), 1433–1438.

Braaten, J. T., Wood, P. J., Scott, F. W., Wolynetz, M. S., Lowe, M. K., Bradley-White, P., et al. (1994). Oat β-glucan reduces blood cholesterol concentration in hypercholesterolaemic subjects. *European Journal of Clinical Nutrition*, *48*, 465–474.

British Standards Institution (1970). *Methods for the determination of specific surface area of powders. British Standards 4359, Part 3*. London: British Standards Institution.

Carlson, W. A., Ziengenfuss, E. M., & Overton, J. D. (1962). Compatibility and manipulation of guar gum. *Food Technology*, *16*, 50–54.

Chourasia, M. K., & Jain, S. K. (2004). Potential of guar gum microspheres for target specific drug release to colon. *Journal of Drug Targeting*, *12*, 435–442.

Ellis, P. R., Dawoud, F. M., & Morris, E. R. (1991). Blood-glucose, plasma-insulin and sensory responses to guar-containing wheat breads—Effects of molecular-weight and particle-size of guar gum. *British Journal of Nutrition*, *66*, 363–379.

Ellis, P. R., & Morris, E. R. (1991). Importance of the rate of hydration of pharmaceutical preparations of guar gum—A new in vitro monitoring method. *Diabetic Medicine*, *8*, 378–381.

Ellis, P. R., Morris, E. R., & Low, A. G. (1986). Guar gum—The importance of reporting data on its physicochemical properties. *Diabetic Medicine*, *3*, 490–491.

Ellis, P. R., Roberts, F. G., Low, A. G., & Morgan, L. M. (1995). The effect of high-molecular-weight guar gum on net apparent glucose-absorption and net apparent insulin and gastric-inhibitory polypeptide production in the growing pig—Relationship to rheological changes in jejunal digesta. *British Journal of Nutrition*, *74*, 539–556.

Ellis, P. R., Wang, Q., Rayment, P., Ren, Y., & Ross-Murphy, S. B. (2001). Guar gum—Agricultural and botanical aspects, physicochemical and nutritional properties, and its use in the development of functional foods. In S. S. Cho, & M. Dreher (Eds.), *Handbook of dietary fiber* (pp. 613–657). New York, NY: Marcel Dekker.

Englyst, H. N., Quigley, M. E., Hudson, G. J., & Cummings, J. H. (1992). Determination of dietary fiber as nonstarch polysaccharides by gas–liquid-chromatography. *Analyst*, *117*, 1707–1714.

Friend, D. R. (2005). New oral delivery systems for treatment of inflammatory bowel disease. *Advanced Drug Delivery Reviews*, *375*(57), 247–265.

Goel, N., Shah, S. N., & Asadi, M. (2000). New empirical correlation to predict apparent viscosity of borate-crosslinked guar gel in fractures. *Spe Production and Facilities*, *15*, 90–95.

Guo, J. H., Skinner, G. W., Harcum, W. W., & Barnum, P. E. (1998). Pharmaceutical applications of naturally occurring water-soluble polymers. *Pharmaceutical Science and Technology Today*, *1*, 254–261.

Jelinek, Z. K. (1974). *Particle size analysis*. Chichester, UK: Ellis Horwood.

Jenkins, D. J. A., Wolever, T. M. S., Leeds, A. R., Gassull, M. A., Haisman, P., Dilawari, J., et al. (1978). Dietary fibers, fiber analogs, and glucose-tolerance—Importance of viscosity. *British Medical Journal*, *1*, 1392–1394.

Joint Formulary Committee (2005). *British national formulary*. London, UK: British Medical Association and Royal Pharmaceutical Society of Great Britain.

Kesavan, S., & Prudhomme, R. K. (1992). Rheology of guar and HPG cross-linked by borate. *Macromolecules*, *25*, 2026–2032.

Lauer, O. (1966). *Grain size measurements on commercial powders—A guide for experts*. Ausberg, Germany: Alpine, Ausberg.

Montejo, C., Barcia, E., Fernandez-Carballido, A., & Molina-Martinez, I. T. (2004). Time delay avoids interaction between guar gum and sulphadiazine after oral administration. *Journal of Drug Delivery Science and Technology*, *14*, 395–399.

O'Connor, N., Tredger, J., & Morgan, L. (1981). Viscosity differences between various guar gums. *Diabetologia*, *20*, 612–615.

Patrick, P. G., Gohman, S. M., Marx, S. C., DeLegge, M. H., & Greenberg, N. A. (1998). Effect of supplements of partially hydrolyzed guar gum on the occurrence of constipation and use of laxative agents. *Journal of the American Dietetic Association*, *98*, 912–914.

Perez, R. M., Siquier, S., Ramirez, N., Muller, A. J., & Saez, A. E. (2004). Non-Newtonian annular vertical flow of sand suspensions in aqueous solutions of guar gum. *Journal of Petroleum Science and Engineering*, *44*, 317–331.

Rayment, P., Ross-Murphy, S. B., & Ellis, P. R. (1995). Rheological properties of guar galactomannan and rice starch mixtures. 1. Steady shear measurements. *Carbohydrate Polymers*, *28*, 121–130.

Robinson, G., Ross-Murphy, S. B., & Morris, E. R. (1982). Viscosity molecular-weight relationships, intrinsic chain flexibility, and dynamic solution properties of guar galactomannan. *Carbohydrate Research*, *107*, 17–32.

Schneider, R., & Sostar-Turk, S. (2003). Good quality printing with reactive dyes using guar gum and biodegradable additives. *Dyes and Pigments*, *57*, 7–14.

Slavin, J. L., & Greenberg, N. A. (2003). Partially hydrolyzed guar gum: Clinical nutrition uses. *Nutrition*, *19*, 549–552.

To, K. M., Mitchell, J. R., Hill, S. E., Bardon, L. A., & Matthews, P. (1994). Measurement of hydration of polysaccharides. *Food Hydrocolloids*, *8*, 243–249.

Turk, S. S., & Schneider, R. (2000). Printing properties of a high substituted guar gum and its mixture with alginate. *Dyes and Pigments*, *47*, 269–275.

US Food and Drug Administration (1994). *A food labeling guide—Appendix C: Health claims*. Rockville, MD, USA: US FDA.

Wang, Q., Ellis, P. R., & Ross-Murphy, S. B. (2000). The stability of guar gum in an aqueous system under acidic conditions. *Food Hydrocolloids*, *14*, 129–134.

Wang, Q., Ellis, P. R., & Ross-Murphy, S. B. (2002). Dissolution kinetics of guar gum powders. I. Methods for commercial polydisperse samples. *Carbohydrate Polymers*, *49*, 131–137.

Wang, Q., Ellis, P. R., & Ross-Murphy, S. B. (2003). Dissolution kinetics of guar gum powders—II. Effects of concentration and molecular weight. *Carbohydrate Polymers*, *53*, 75–83.

Whister, R. L., & Hymowitz, T. (1979). *Guar: Agronomy, production, industrial use and nutrition*. West Lafayette, IN: Purdue University Press.

Wood, P. J., Braaten, J. T., Scott, F. W., Riedel, K. D., Wolynetz, M. S., & Collins, M. W. (1994). Effect of dose and modification of viscous properties of oat gum on plasma–glucose and insulin following an oral glucose-load. *British Journal of Nutrition*, *72*, 731–743.

Zhou, Y. X., & Shah, S. N. (2004). Rheological properties and frictional pressure loss of drilling, completion, and stimulation fluids in coiled tubing. *Journal of Fluids Engineering-Transactions of the ASME*, *126*, 153–161.